Nanoscale

Accepted Manuscript

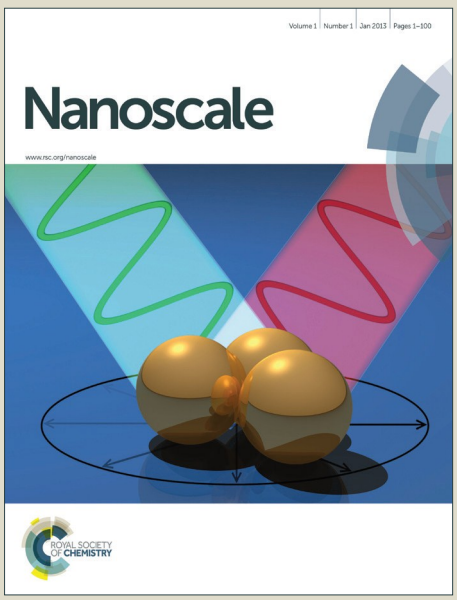

ROYAL SOCIETY OF CHEMISTRY

www.rsc.org/nanoscale

Interface Engineering: Broadband Light and Low Temperature Gas Detection Abilities by Using Nano-Heterojunction Device

*Chien-Min Chang, Ching-Han Hsu, Yi-Wei Liu, Tzu-Chiao Chien and Jun-Han Song, Ping-Hung Yeh**

[*] Prof. Ping-Hung Yeh Corresponding-Author,
Department of Physics, Tamkang University, Tamsui, New Taipei City, 25137, Taiwan
E-mail: ((phyeh331@mail.tku.edu.tw))

Abstract

In this research work, we have designed the nano-heterojunction device by using interface defects and band bending effects, which can have broadband light detection (from 365~940 nm) and low operating temperature (50℃) gas detection abilities. The broadband light detection mechanism is because the defects and the band bending between the heterojunction interface. We have demonstrated this mechanism by using $CoSi_2/SnO_2$, $CoSi_2/TiO_2$, Ge/SnO_2 and Ge/TiO_2 nano-heterojunction devices, all above devices show broadband light detection ability. Furthermore, the nano-heterojunction of the nano-device has local Joule-heating effect. For gas detection, the results show that the nano-heterojunction device presents great detection ability. The reset time and sensitivity of nano-heterojunction device are an order faster and larger than the Schottky-contacted devices (previous works[1]); it is due to the local Joule-heating effect between the interface of nano-heterojunction. Based on above idea, we can design widespread used and diversification nano-device.

Keywords: interface defect, UV-visible light detection, low temperature gas detection,

nano-heterojunction

Introduction

Recently, the surface defect of nanomaterials, have been extensively studied and utilized to form nano-devices for different application[2-6]. By utilizing the surface defect, metal-oxide nanometerials, which are quite sensitive for the UV[7,8], gas[9,10] and bio-molecules[11,12] detection. To enhance the performance of metal-oxide nanomaterials, several articles reported using Schottky contact mechanism to form nanogenerators[13-16], piezotronic devices[17-19] and nanosensors[20-23]. For nanosensor, using Schottky contact can improve the sensitivity, response and reset time, that is due to the surface defects can tune the Schottky barrier to vary the current signal so easily[24,25]. So that, the surface defect of metal-oxide nanomaterials is main parameter of nanosensor. The surface defect and the oxygen vacancy of metal-oxide nanomaterials have been reported and discussed widely[26-29]. In this research work, we designed nano-heterojunction devcie by using metal-oxide and semiconductor nanowires to create interface defect and band bending effects for broadband light and low temperature gas detections.

SnO_2 and TiO_2, which have strong potential for ultraviolet (UV) light detection application, that is due to its large band gap[30,31]. Otherwise, SnO_2 and TiO_2 are also candidates for gas detection, because the oxygen vacancy. Furthermore, Ge and $CoSi_2$ are common semiconducting materials; these materials are unconcerned with photo and gas molecules detection. Using these semiconductor materials can figure out the detection mechanism of interface defect between the nano-heterojunction devices, and exclude the materials affection.

Results and discussion

The detail analyses of Ge and SnO_2 can be obtained from the TEM images, the growth direction of Ge and SnO_2 can be identified from the diffraction pattern, high resolution TEM images and EDS element line scan analysis, as shown in Figure 1 (a)~(f). The schematic and current-voltage curve of nano-heterojunction device can be seen in Figure 1 (g). From the I-V curve, we can see a well rectification property and confirm our device has a nano-heterojunction.

The SEM image can show the interface region of the nano-heterojunction device, as illustrated in Figure 2 (a). For photo detection, the broadband light (from 365~940 nm wavelengths light) can be detected by our nano-heterojunction device, as shown in Figure 2 (b). The current variations are decreasing as the wavelength increasing, as shown in Figure 2 (c). For mechanism study, we fabricated simply SnO_2 or Ge nanowire device to compare with our nano-heterojunction device; there is no broadband light detection ability for each simply nanowire device, as shown in Figure S1. So based on these experimental results, we hypothesize that the detection mechanism is due to the interface defect and band bending effects of nano-heterojunction device. The interface between SnO_2/Ge nano-heterojunction has various defects, such as surface defects and oxygen vacancies, which can be the generation centers for photocurrent generating under different wavelengths light illumining; the other reason why the nano-heterojunction has broadband light detection ability is because band bending of the heterojunction, as shown in Figure 2(d). Both interface defects and band bending effects can be the generation sources to generate electron-hole pairs to form the photo current.

For further investigation, we also fabricated other nano-heterojunction ($CoSi_2$/SnO_2,

$CoSi_2/TiO_2$ and Ge/TiO_2) devices to prove the interface defects effect of nano-heterojunction, as shown in Figure 3. All the nano-heterojunction devices have same response/reset time, 20 ms, which is the detection limit of electrical measurement equipment (Agilent B1500). Based on the results, these nano-heterojunction devices all have broadband light detection ability; but different interface defect amounts of each nano-heterojunction device can have various current output level. Using this interface defect as generation centers to have broadband light detection seemed not just restricted within specific nanomaterials; nanomaterials with interface defects mostly can have broadband light detection ability. The sensitivities of each device for various wavelength light can be seen in Figure S2.

From our results, the interface defect is quite sensitive to its surrounding, especially O_2, so we can use this nano-heterojunction device as gas molecules detectors, 50 ppm CO/pure O_2, as seen in Figure 4 (a). Due to the nano-contact, the current density is exceedingly higher between the interface of the nano-heterojunction device, compare with Schottky-contacted device[1]; absolutely high current density can create gigantic local Joule-heating effect between the interface[24]. So the low operating temperature CO detection can be achieved at 50 ℃; compare with the previous works[1] and other typical gas sensor[32-34], they all need more than 150 ℃ to have significant response. Otherwise, at 250 ℃ operating temperature, the reset time and sensitivity of nano-heterojunction device are an order faster and larger than the Schottky-contacted devices[1]; the reset time and sensitivity of nano-heterojunction/Schottky-contacted devices are 2.9 s/30 s and 11238 %/3235 %, respectively. Moreover, because the local Joule-heating effect, the operating temperature can be decreased as using nano-heterojunction device, the reset time and sensitivity of nano-heterojunction device are

5.2 s and 4189 %, respectively, at 150 ℃ operating temperature; which is superior in response and sensitivity compare with the Schottky-contacted devices[1] at 250 ℃ operating temperature. In Figure 4 (b), the response and reset time was reasonable enhanced when the operating temperature increasing. The detail measurements of each temperature are shown in Figure S3.

From our data, the signal of various CO levels can't be differentiated; the reason is because the interface barrier height of nano-heterojunction only need few gas amounts to change. So that when the CO concentraton below such amoumt, like 2 ppm, the moleculers are not enough to absorb on and tune the height of the nano-heterojunction, we can see the current variations of 1 and 2 ppm are not like that above 5 ppm. So for higher gas concentration, the signal output will be saturated, as shown in Figure 4 (c). The reason is because single nano-heterojunction device only has limit area to detect gas amount. But the response and reset time will be enhanced when CO concentration increasing, as seen in Figure 4 (d). The mechanism why nano-heterojunction device can have outstanding gas detection property can be explained in Figure 5, compare with Schottky-contacted device[1]. Firstly, it just needs fewer gas molecules to switch the interface barrier, as shown in Figure 5 (b); only needs few O_2 molecules, the interface barrier height can be increased to have low current output, as shown in Figure 5(a). For CO sensing, it also just needs few CO molecules to low the interface barrier height to have increasing current, as shown in Figure 5 (c). Secondly, the local Joule-heating can increase the interface temperature to assist with gas absorption at heterojunction interface. This single nano-heterojunction device might not monitor different CO levels, but if we can put nano-heterojunction devices in parallel to enhance the gas monitor level distinguishability, just like previous work[24]. For commercial application, we can redesign the device structure, such as

using Ge and SnO2 NWs layers to create tons of nano-heterojunction as a gas detector, then the different gas level can be detected. But in this article, we just focus to clarify the interface defect effect, try to give a further investigation.

Experiment

Fabrication of the nano-heterojunction devices

The nano-heterojunction was formed by different nanowires by free contact; the other side of each nanowire is placed on Pt electrode and using focus ion beam (FIB) system to deposit Pt:Ga to form Ohmic contact[1,23]. The operating bias of nano-heterojunction devices are from -1.5 V~ -5 V and the measurement system is a chamber with heating stage, electrical probes, gas flow and pump, as shown in Figure S4.

Fabrication of the SnO_2 nanowires

The SnO_2 NWs were synthesized on silicon substrates at 850 ℃ via the general catalyst free thermal evaporation method using SnO_2 and carbon powders as sources in a horizontal quartz tube connected to a mass flow controller (MFC) and a vacuum pump. The source was placed at the high temperature zone 1000 ^{o}C, the Si substrates then positioned in the source downstream. After the tube had been sealed and evacuated to the base pressure, a carrier gas, Ar/O_2 (100 sccm), was kept flowing through the tube to direct the deposition process for 4.5 h.

Fabrication of the TiO_2 nanowires

The preparation of single crystalline TiO_2 NWs were used a suitable amount of TiO_2 powders, serving as the precursor, that was placed at the center of an alumina tube. The alumina tube is situated in a furnace to serve as the reaction chamber. Using Ar, as the carrier gas, at a flow rate of 50 sccm flows through the alumina tube to transport the TiO_2 vapors downstream for the NW growth.

The furnace was heated to 1475 ℃ and held at that temperature for 4.5 h under ~250 mbar. After the NW growth, the tube was cooled under Ar flow.

Fabrication of the Ge nanowires

The preparation of single crystalline Ge NWs followed H.-Y. Tuan's work[35]. DPG solution in 300 mM was loaded into a 10 ml loop and was injected into the reactor. When a reaction reached the end of the injection, another stock solution was loaded into the loop and was injected to reactor to continue the nanowire synthesis. For 0.2 g nanowire synthesis, three successive injections, equal to a total of 30 ml DPG solution (300 mM), were injected into the reactor. Prior to the alkanethiol reactions of Ge nanowires, the nanowire product was cleaned by immersion of nanowires in a 1 : 1 volume mixture of toluene and ethanol, followed by centrifugation at 8000 rpm for 5 min to remove unreacted reactants. Hydrideterminated nanowires were produced by immersion in aqueous 5% HF for 5 min, followed by an anhydrous methanol rinse. The etched wires were then quickly transferred to a Schlenk line under Ar atmosphere. 5 ml of neat alkanethiol (1-hexanethiol, 1-dodecanethiol or 1-hexadecanethiol) was added to immerse Ge nanowires. The mixed solution was heated to 80℃ for 24 h for thiolation. Afterwards, the nanowire product was dispersed in a 1 : 1 : 1 volume mixture of chloroform, toluene, and ethanol for centrifugation at 8000 rpm for 5 min. The washing procedure was repeated twice more to remove excess organic ligands. A Ge nanowire fabric was made by vacuum-filtering a dispersion of nanowires in toluene (0.5–1 mg ml^{-1}) through porous alumina filters (Whatman Anodisc13, 0.2 mm pores). The fabric was air-dried for 2 h, and then was removed by careful peeling or dissolving the filtration membrane.

Fabrication of the $CoSi_2$ nanowires

The preparation of single crystalline $CoSi_2$ NWs followed the procedures presented in a previous work[36]. Single crystal Si wafers were used as substrates. Prior to the loading into the two-zone furnace at the atmosphere pressure with an Ar flow. The samples were placed at the downstream and the cobalt chloride powder at the upstream. The powders were heated at 600 ℃ and the heating zone was set at temperatures of 900 ℃ downstream. The two heating centers were at a distance of 20 cm apart. The precursor vapors were carried by the Ar flow, which was set at 300 sccm, and reacted with silicon substrates placed downstream for 2 h unless otherwise mentioned. The furnace was then allowed to cool to room temperature.

Conclusions

In this research work, we have demonstrated that the nano-heterojunction devices can have broadband light detection ability (from 365~940 nm). The mechanism is because the defects and the band bending effects between the heterojunction interface. We have demonstrated this mechanism by using $CoSi_2/SnO_2$, $CoSi_2/TiO_2$, Ge/SnO_2 and Ge/TiO_2 nano-heterojunction devices, all above devices show broadband light detection ability. Besides, the nano-heterojunction device is very sensitive to its surrounding environment; because the interface defects can affect the photo detection ability. So we used the CO/O_2 alternate-detection to verify our hypothesis, and the results show that the nano-heterojunction device presents great detection ability. The reset time and sensitivity of

nano-heterojunction device are an order faster and larger than the Schottky-contacted devices, which is due to the local Joule-heating effect between the interface of nano-heterojunction; because the local Joule-heating effect, the operating temperature can be reduced to 50 ℃. We verify that the nano-heterojunction device can achieve broadband light and low operating temperature gas detection abilities based on the interface defects and band bending effects. Based on above idea, we can design widespread used and diversification nano-device.

Acknowledgements

This research was supported by the National Science Council of the Republic of China (Taiwan) under grants NSC-101-2112-M-032-004-MY3.

Figures

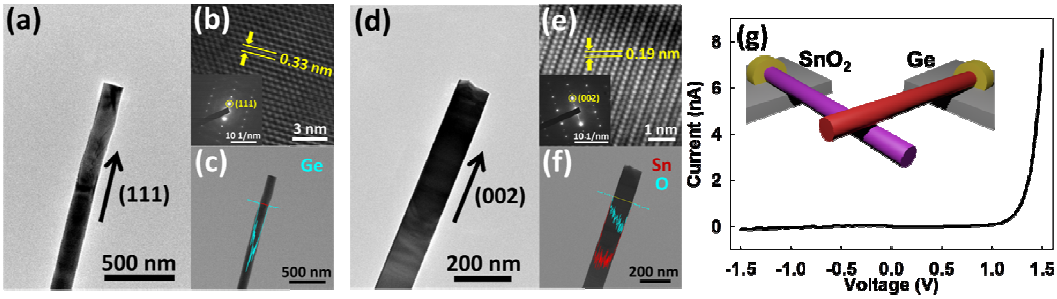

Figure 1. (a) Low magnification TEM image of Ge nanostructure with the growth orientation (111). (b) and (c) show the lattice constant and EDS element line scan analysis of Ge. (d) Low magnification TEM image of SnO_2 nanostructure with the growth orientation (002). (e) and (f) show

the lattice constant and EDS element line scan analysis of SnO_2. (g) Schematic diagram and I-V curve of SnO_2/Ge nano-heterojunction device.

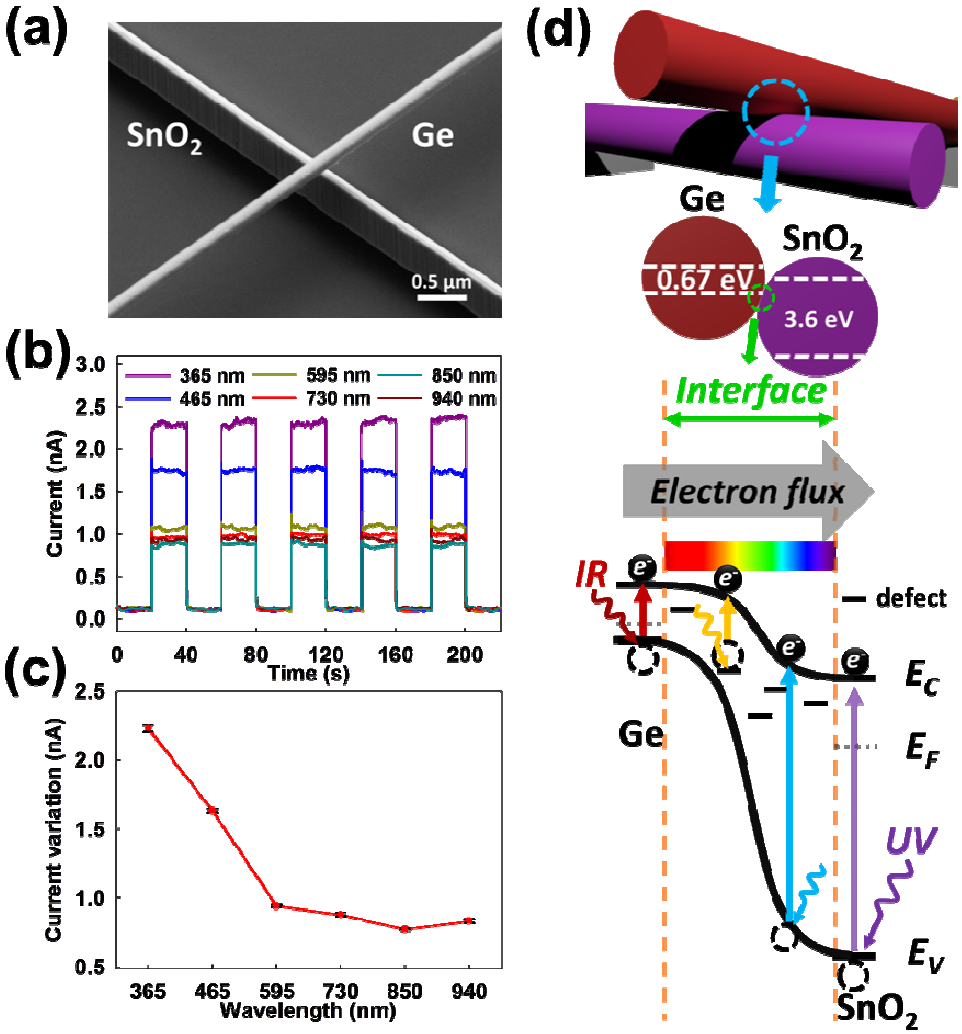

Figure 2. (a) The SEM image of SnO_2/Ge nano-heterojunction device. (b) The broadband light (UV-visible light) detection can achieved at reversed bias (1.5 V). (c) The current variation of photo detection under different wavelengths illuminating. (d) The broadband light sensing mechanism diagrams of SnO_2/Ge nano-heterojunction device. The interface defects and band bending between SnO_2/Ge nano-heterojunction can be the generation centers under different wavelengths light illuminating.

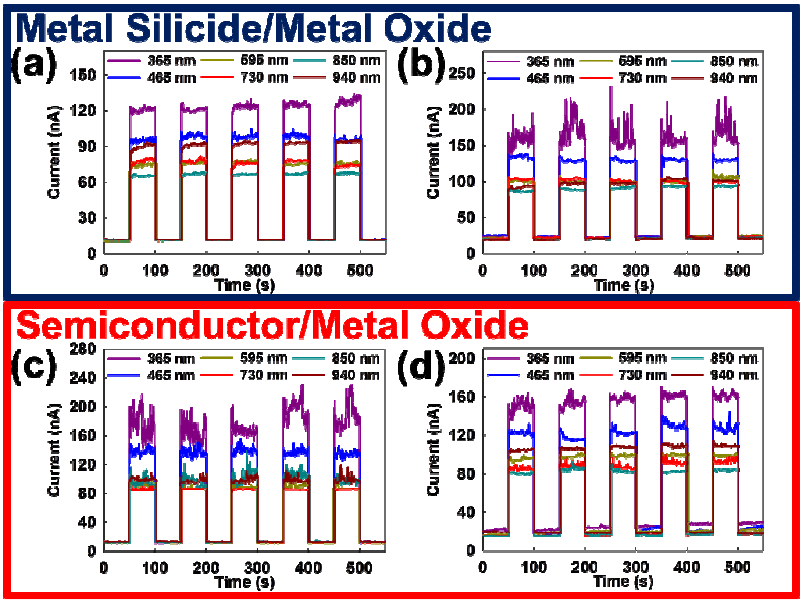

Figure 3. Show the broadband light detection properties of nano-Schottky and nano-heterojunction structure (a) and (b) represent the photo detection properties of $CoSi_2/SnO_2$ and $CoSi_2/TiO_2$ nano-Schottky devices. (c) and (d) represent the photo detection properties of Ge/SnO_2 and Ge/TiO_2 nano- heterojunction devices. All devices were measured at reversed bias (5 V).

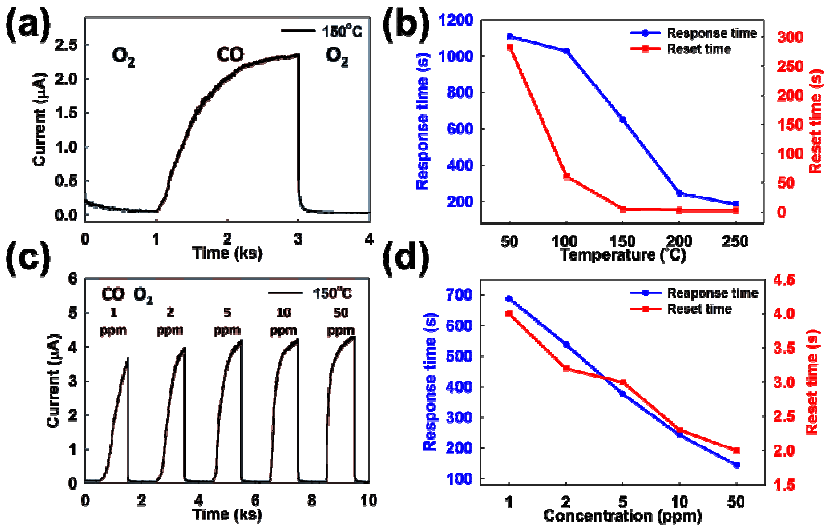

Figure 4. The gas detection ability can be seen. (a) show the 50 ppm CO detection ability at 150 ℃. (b) The response and reset time of the 50 ppm CO detection can be improved by increasing operation temperature. (c) Various CO concentration detection ability can be seen at 150 ℃. The current variations were similar above 5 ppm CO concentration, that is an evidence to verify the detection area is just the nano-heterojunction region. (d) The response and reset time of the various CO detections can be seen at 150 ℃.

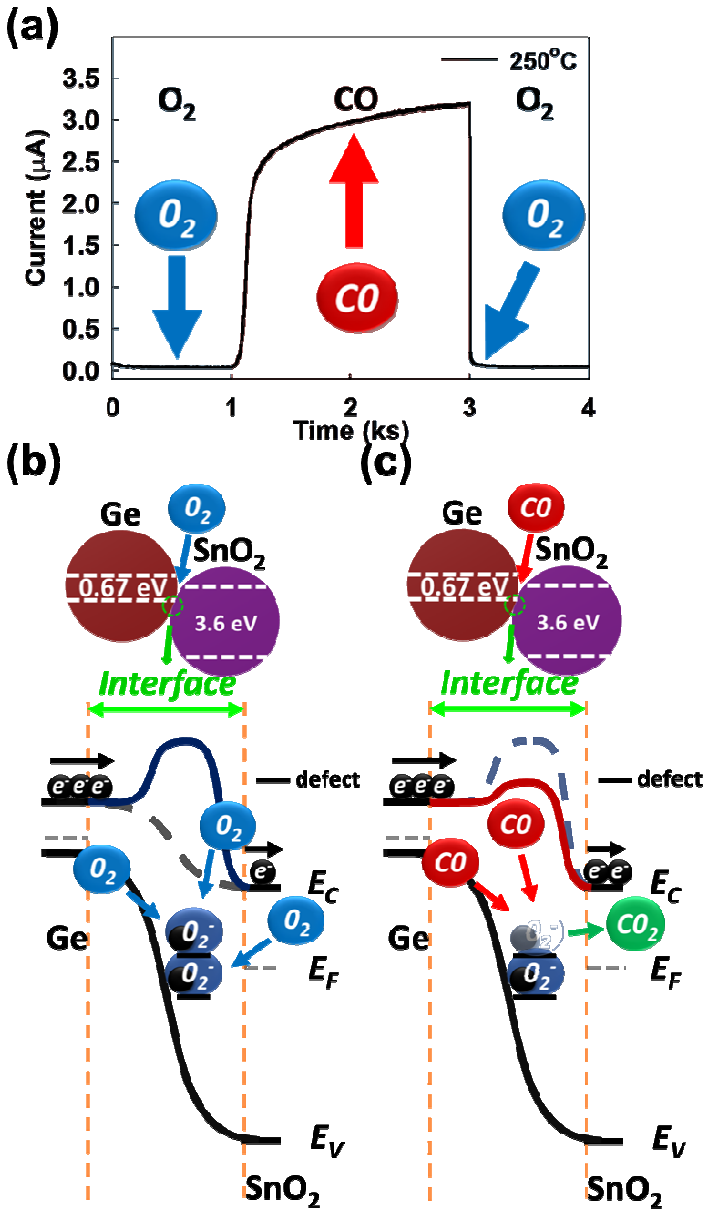

Figure 5 represents the gas detection ability and detection mechanism. (a) The 50 ppm CO detection ability at 250 ℃ can be seen. (b) For O_2 detection mechanism, the O_2 absorbed on the surface of SnO_2, between the interface of SnO_2/Ge to form O_2^-, can increase the interface barrier height; so the nano-heterojunction device has low current output. (c) As the CO flow in, the CO can remove the O_2^- and reduce the interface barrier height; the nano-heterojunction device will have increasing current output as more CO absorption.

References

1 T.-Y. Wei, P.-H. Yeh, S.-Y. Lu and Z. L. Wang, *J. Am. Chem. Soc.*, 2009, **131**, 17690-17695.

2 C.-Y. Lai, T.-C. Chien, T.-Y. Lin, T. Ke, S.-H. Hsu, Y.-J. Lee, C.-y. Su, J.-T. Sheu and P.-H. Yeh, *Nanoscale Res. Lett.*, 2014, **9**, 281-281.

3 Kenry and C. T. Lim, *Prog. Mater Sci.*, 2013, **58**, 705-748.

4 S. Mao, S. Cui, K. Yu, Z. Wen, G. Lu and J. Chen, *Nanoscale*, 2012, **4**, 1275-1279.

5 C. Zhang, W. Tian, Z. Xu, X. Wang, J. Liu, S.-L. Li, D.-M. Tang, D. Liu, M. Liao, Y. Bando and D. Golberg, *Nanoscale*, 2014, **6**, 8084-8090.

6 Z. Zhao, J. Tian, Y. Sang, A. Cabot and H. Liu, *Adv. Mater.*, 2015, **27**, 2557-2582.

7 A. Littig, H. Lehmann, C. Klinke, T. Kipp and A. Mews, *ACS Appl. Mater. Interfaces*, 2015, **7**, 12184-12192.

8 S. C. Rai, K. Wang, Y. Ding, J. K. Marmon, M. Bhatt, Y. Zhang, W. Zhou and Z. L. Wang, *ACS Nano*, 2015, **9**, 6419-6427.

9 D. Yang, M. K. Fuadi, K. Kang, D. Kim, Z. Li and I. Park, *ACS Appl. Mater. Interfaces*, 2015, **7**, 10152-10161.

10 I. Fratoddi, A. Macagnano, C. Battocchio, E. Zampetti, I. Venditti, M. V. Russo and A. Bearzotti, *Nanoscale*, 2014, **6**, 9177-9184.

11 Y. Zhao, P. Deng, Y. Nie, P. Wang, Y. Zhang, L. Xing and X. Xue, *Biosens Bioelectron*, 2014, **57**, 269-275.

12 A. Choi, K. Kim, H.-I. Jung and S. Y. Lee, *Sens. Actuators, B*, 2010, **148**, 577-582.

13 Y. Wu, Q. Jing, J. Chen, P. Bai, J. Bai, G. Zhu, Y. Su and Z. L. Wang, *Adv. Funct. Mater.*, 2015, **25**, 2166-2174.

14 L. W. Yamin, in *Piezoelectric ZnO Nanostructure for Energy Harvesting*, John Wiley & Sons, Inc., 2015, ch. 4, pp. 65-103.

15 S. Garain, T. K. Sinha, P. Adhikary, K. Henkel, S. Sen, S. Ram, C. Sinha, D. Schmeißer and D. Mandal, *ACS Appl. Mater. Interfaces*, 2015, **7**, 1298-1307.

16 W. Seung, M. K. Gupta, K. Y. Lee, K.-S. Shin, J.-H. Lee, T. Y. Kim, S. Kim, J. Lin, J. H. Kim and S.-W. Kim, *ACS Nano*, 2015.

17 Z. L. Wang, in *Piezotronics and Piezo-Phototronics*, Springer Berlin Heidelberg, 2012, ch. 1, pp. 1-17.

18 R. Yu, S. Niu, C. Pan and Z. L. Wang, *Nano Energy*, 2015, **14**, 312-339.

19 R. Yu, C. Pan, J. Chen, G. Zhu and Z. L. Wang, *Adv. Funct. Mater.*, 2013, **23**, 5868-5874.

20 S. Niu, Y. Hu, X. Wen, Y. Zhou, F. Zhang, L. Lin, S. Wang and Z. L. Wang, *Adv. Mater.*, 2013, **25**, 3701-3706.

21 J. Zhou, Y. Gu, Y. Hu, W. Mai, P.-H. Yeh, G. Bao, A. K. Sood, D. L. Polla and Z. L. Wang, *Appl. Phys. Lett.*, 2009, **94**, 191103.

22 C. Pan, R. Yu, S. Niu, G. Zhu and Z. L. Wang, *ACS Nano*, 2013, **7**, 1803-1810.

23 Y. Hu, J. Zhou, P.-H. Yeh, Z. Li, T.-Y. Wei and Z. L. Wang, *Adv. Mater.*, 2010, **22**, 3327-3332.

24 C.-H. Sung, T.-C. Chien, C.-M. Chang, C.-M. Chang and P.-H. Yeh, *RSC Adv.*, 2015, **5**, 16769-16773.

25 J. K. Hsu, T. Y. Lin, C. Y. Lai, T. C. Chien, J. H. Song and P. H. Yeh, *Appl. Phys. Lett.*, 2013, **103**, 123507.

26 Y. Zhang, A. Kolmakov, S. Chretien, H. Metiu and M. Moskovits, *Nano Lett.*, 2004, **4**, 403-407.

27 R. Gurwitz, R. Cohen and I. Shalish, *J. Appl. Phys.*, 2014, **115**, 033701.

28 J. Pan, R. Ganesan, H. Shen and S. Mathur, *J. Phys. Chem. C*, 2010, **114**, 8245-8250.

29 A. Kar, S. Kundu and A. Patra, *J. Phys. Chem. C*, 2010, **115**, 118-124.

30 W. Zhou, Y. Liu, Y. Yang and P. Wu, *J. Phys. Chem. C*, 2014, **118**, 6448-6453.

31 J. Zou, Q. Zhang, K. Huang and N. Marzari, *J. Phys. Chem. C*, 2010, **114**, 10725-10729.

32 I. Giebelhaus, E. Varechkina, T. Fischer, M. Rumyantseva, V. Ivanov, A. Gaskov, J. R. Morante, J. Arbiol, W. Tyrra and S. Mathur, *J. Mater. Chem. A*, 2013, **1**, 11261-11268.

33 E. N. Dattoli, A. V. Davydov and K. D. Benkstein, *Nanoscale*, 2012, **4**, 1760-1769.

34 H. Huang, C. Y. Ong, J. Guo, T. White, M. S. Tse and O. K. Tan, *Nanoscale*, 2010, **2**, 1203-1207.

35 H.-J. Yang and H.-Y. Tuan, *J. Mater. Chem.*, 2012, **22**, 2215-2225.

36 C.-I. Tsai, P.-H. Yeh, C.-Y. Wang, H.-W. Wu, U.-S. Chen, M.-Y. Lu, W.-W. Wu, L.-J. Chen and Z.-L. Wang, *Cryst. Growth Des.*, 2009, **9**, 4514-4518.

Title: Interface Engineering: Broadband Light and Low Temperature Gas Detection Abilities by Using Nano-Heterojunction Device

ToC figure: By using the interface defect, band bending and nano-contact effects, the broadband light and low temperature gas detection abilities can be achieved as a nano-heterojunction device.